An EPR experiment testing the non-separability of the $K^0\overline{K^0}$ wave function

A. Apostolakis, E. Aslanides, G. Backenstoss, P. Bargassa, O. Behnke, A. Benelli, V. Bertin, F. Blanc, P. Bloch, P. Carlson, et al.

EUROPEAN ORGANIZATION FOR NUCLEAR RESEARCH

CERN–PPE/97–140
October 10, 1997

An EPR experiment testing the non-separability of the $\mathrm{K}^0\overline{\mathrm{K}}^0$ wave function

CPLEAR Collaboration

A. Apostolakis[1)], E. Aslanides[11)], G. Backenstoss[2)], P. Bargassa[13)], O. Behnke[17)], A. Benelli[9)], V. Bertin[11)], F. Blanc[7,13)], P. Bloch[4)], P. Carlson[15)], M. Carroll[9)], E. Cawley[9)], G. Chardin[14)], M.B. Chertok[3)], A. Cody[9)], M. Dejardin[14)], J. Derre[14)], A. Ealet[11)], C. Eleftheriadis[16)], R. Ferreira-Marques[5)], W. Fetscher[17)], M. Fidecaro[4)], A. Filipčič[10)], D. Francis[3)], J. Fry[9)], E. Gabathuler[9)], R. Gamet[9)], H.-J. Gerber[17)], A. Go[14)], C. Guyot[14)], A. Haselden[9)], P.J. Hayman[9)], F. Henry-Couannier[11)], R.W. Hollander[6)], E. Hubert[11)], K. Jon-And[15)], P.-R. Kettle[13)], C. Kochowski[14)], P. Kokkas[4)], R. Kreuger[6)], R. Le Gac[11)], F. Leimgruber[2)], I. Mandić[10)], N. Manthos[8)], G. Marel[14)], M. Mikuž[10)], J. Miller[3)], F. Montanet[11)], A. Muller[14)], T. Nakada[13)], B. Pagels[17)], I. Papadopoulos[16)], P. Pavlopoulos[2)], A. Policarpo[5)], G. Polivka[2)], R. Rickenbach[2)], B.L. Roberts[3)], T. Ruf[4)], M. Schäfer[17)], L.A. Schaller[7)], T. Schietinger[2)], A. Schopper[4)], P. Schune[14)], L. Tauscher[2)], C. Thibault[12)], F. Touchard[11)], C. Touramanis[9)], C.W.E. Van Eijk[6)], S. Vlachos[2)], P. Weber[17)], O. Wigger[13)], M. Wolter[17)], C. Yeche[14)], and D. Zavrtanik[10)].

Abstract

The EPR-type strangeness correlation in the $\mathrm{K}^0\overline{\mathrm{K}}^0$ system produced in the reaction $\overline{\mathrm{p}}\mathrm{p} \to \mathrm{K}^0\overline{\mathrm{K}}^0$ at rest has been tested using the CPLEAR detector. The strangeness was tagged via strong interaction with absorbers away from the creation point. The results are consistent with the QM non-separability of the wave function and exclude a spontaneous wave-function factorisation at creation (CL $> 99.99\%$).

(Submitted to Physics Letters B)

[1)] University of Athens, Greece
[2)] University of Basle, Switzerland
[3)] Boston University, USA
[4)] CERN, Geneva, Switzerland
[5)] LIP and University of Coimbra, Portugal
[6)] Delft University of Technology, Netherlands
[7)] University of Fribourg, Switzerland
[8)] University of Ioannina, Greece
[9)] University of Liverpool, UK
[10)] J. Stefan Inst. and Phys. Dep., University of Ljubljana, Slovenia
[11)] CPPM, IN2P3-CNRS et Université d'Aix-Marseille II, France
[12)] CSNSM, IN2P3-CNRS, Orsay, France
[13)] Paul Scherrer Institut (PSI), Switzerland
[14)] CEA, DSM/DAPNIA, CE-Saclay, France
[15)] Royal Institute of Technology, Stockholm, Sweden
[16)] University of Thessaloniki, Greece
[17)] ETH-IPP Zürich, Switzerland

1 Introduction

According to Quantum Mechanics (QM), if a pair of particles is created by any kind of interaction, the two-particle wave function retains its non-separable character even if the particles are space-like separated. This feature leads to puzzling non-local correlations between the observed properties of the two particles. A measurement of a given parameter for one particle, undetermined prior to the measurement, may predict with certainty the outcome of a measurement on the second particle.

This apparent difficulty of QM, pointed out in 1935 by Einstein, Podolsky and Rosen and known as the EPR paradox [1], gave rise to an animated debate over the past sixty years. In 1936, Furry [2] discussed a spontaneous factorization of the two-body wave function immediately after the creation of the particle pair. Following an older idea [3], it was suggested [1, 4] that there may exist supplementary variables ('hidden variables') outside the scope of QM which determine the results of individual measurements. In 1964, J.S. Bell [5] showed that the whole class of local hidden-variables models leads to an inequality (Bell's inequality) violated by QM under certain special conditions. This opened the possibility of experimental tests discriminating between QM and local hidden-variable models [6].

Numerous experiments were performed, mostly measurements of polarization correlation within photon pairs generated in radiative atomic cascade transitions [7, 8], or, more recently, down-conversions [9, 10]. All significant results appear to violate Bell's inequality and are generally interpreted as a confirmation of QM and as a rebuttal of local hidden-variable models.

In particle physics, the strangeness in the $\mathrm{K}^0\overline{\mathrm{K}}^0$ system at creation is analogous to the polarization in the two-photon system. In addition, the strangeness is time-dependent because of the $\mathrm{K}^0 \rightleftarrows \overline{\mathrm{K}}^0$ oscillation. Owing to the fast decrease of the K^0 and $\overline{\mathrm{K}}^0$amplitudes, it is not possible to find an experimental set-up for testing Bell's inequality [11]. But the entanglement of the $\mathrm{K}^0\overline{\mathrm{K}}^0$ wave function before measurement can be tested experimentally. The $J^{PC} = 1^{--}$ $\mathrm{K}^0\overline{\mathrm{K}}^0$ antisymmetric state, as pointed out by several authors [12–16], is well suited for testing this feature through the measurement of the strangeness correlation. The $\overline{\mathrm{p}}\mathrm{p}$ annihilation at rest into $\mathrm{K}^0\overline{\mathrm{K}}^0$ allows such a test to be performed in a convenient way (Section 3).

2 The $\mathrm{K}^0\overline{\mathrm{K}}^0$ system

A $\mathrm{K}^0\overline{\mathrm{K}}^0$ pair, created in a $J^{PC} = 1^{--}$ state, antisymmetric under C and P, is described at kaon proper times $t_\mathrm{a} = t_\mathrm{b} = 0$ by the wave functions Ψ:

$$|\Psi(0,0)\rangle = \frac{1}{\sqrt{2}}[|\mathrm{K}^0(0)\rangle_\mathrm{a}|\overline{\mathrm{K}}^0(0)\rangle_\mathrm{b} - |\overline{\mathrm{K}}^0(0)\rangle_\mathrm{a}|\mathrm{K}^0(0)\rangle_\mathrm{b}], \text{ or}$$

$$|\Psi(0,0)\rangle = \frac{1}{\sqrt{2}}[|\mathrm{K_S}(0)\rangle_\mathrm{a}|\mathrm{K_L}(0)\rangle_\mathrm{b} - |\mathrm{K_L}(0)\rangle_\mathrm{a}|\mathrm{K_S}(0)\rangle_\mathrm{b}]. \quad (1)$$

Here a and b denote either of the two neutral kaons and CP violation has been neglected. The two neutral kaons fly in opposite directions in their centre-of-mass system. The two-body wave function depends on time as

$$|\Psi(t_\mathrm{a},t_\mathrm{b})\rangle = \frac{1}{\sqrt{2}}[|\mathrm{K_S}(0)\rangle_\mathrm{a}|\mathrm{K_L}(0)\rangle_\mathrm{b}\mathrm{e}^{-\mathrm{i}(\alpha_\mathrm{S}t_\mathrm{a}+\alpha_\mathrm{L}t_\mathrm{b})} - |\mathrm{K_L}(0)\rangle_\mathrm{a}|\mathrm{K_S}(0)\rangle_\mathrm{b}\mathrm{e}^{-\mathrm{i}(\alpha_\mathrm{L}t_\mathrm{a}+\alpha_\mathrm{S}t_\mathrm{b})}], \quad (2)$$

where $\alpha_{\mathrm{S,L}} = m_{\mathrm{S,L}} - \mathrm{i}\gamma_{\mathrm{S,L}}/2$, $m_{\mathrm{S,L}}$ and $\gamma_{\mathrm{S,L}}$ being the $\mathrm{K_{S,L}}$ masses and decay widths, respectively. The time dependence for the intensities of events with like- and unlike-strangeness particles is obtained from Eq. (2), with $\Delta m = m_\mathrm{L} - m_\mathrm{S},\ \gamma = (\gamma_\mathrm{S} + \gamma_\mathrm{L})/2$, as follows:

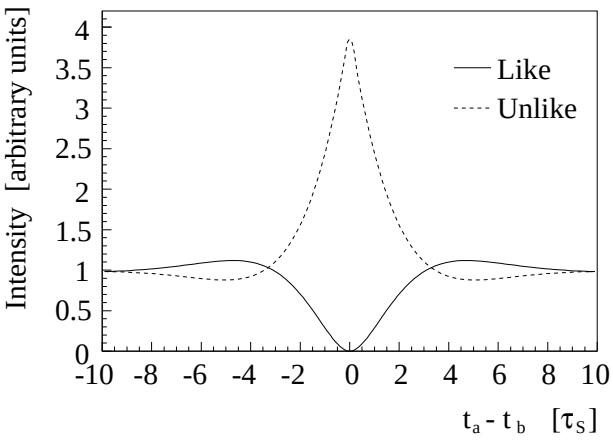

Figure 1: QM correlation for $J^{PC} = 1^{--}$ like- and unlike-strangeness final states as a function of ($t_{\rm a}$- $t_{\rm b}$).

– $J^{PC} = 1^{--}$, like-strangeness events ($\mathrm{K^0K^0}$ or $\overline{\mathrm{K}}^0\overline{\mathrm{K}}^0$),

$$I_{\rm like}(t_{\rm a},t_{\rm b}) = \frac{1}{8}\{{\rm e}^{-(\gamma_{\rm L}t_{\rm a}+\gamma_{\rm S}t_{\rm b})} + {\rm e}^{-(\gamma_{\rm S}t_{\rm a}+\gamma_{\rm L}t_{\rm b})} - 2{\rm e}^{-\gamma(t_{\rm a}+t_{\rm b})}\cos[\Delta m(t_{\rm a}-t_{\rm b})]\}; \quad (3)$$

– $J^{PC} = 1^{--}$, unlike-strangeness events ($\mathrm{K^0}\overline{\mathrm{K}}^0$ or $\overline{\mathrm{K}}^0\mathrm{K^0}$),

$$I_{\rm unlike}(t_{\rm a},t_{\rm b}) = \frac{1}{8}\{{\rm e}^{-(\gamma_{\rm L}t_{\rm a}+\gamma_{\rm S}t_{\rm b})} + {\rm e}^{-(\gamma_{\rm S}t_{\rm a}+\gamma_{\rm L}t_{\rm b})} + 2{\rm e}^{-\gamma(t_{\rm a}+t_{\rm b})}\cos[\Delta m(t_{\rm a}-t_{\rm b})]\}. \quad (4)$$

The coherent addition of the two amplitudes from Eq. (2) generates a time-dependent interference term which has opposite sign for like- and unlike-strangeness states. For identical strangeness at identical times the intensity vanishes and the interference becomes entirely destructive. Therefore the two kaons cannot appear in identical strangeness states at any equal proper time. This is an EPR-type correlation — the measurement of the strangeness of one kaon predicts with certainty the strangeness state of the other unmeasured kaon.

The following asymmetry derived from Eqs. (3) and (4) is a direct measurement of the interference, even if CP is violated:

$$A(t_{\rm a},t_{\rm b}) = \frac{I_{\rm unlike}(t_{\rm a},t_{\rm b}) - I_{\rm like}(t_{\rm a},t_{\rm b})}{I_{\rm unlike}(t_{\rm a},t_{\rm b}) + I_{\rm like}(t_{\rm a},t_{\rm b})} = \frac{2{\rm e}^{-\gamma(t_{\rm a}+t_{\rm b})}\cos[\Delta m(t_{\rm a}-t_{\rm b})]}{{\rm e}^{-(\gamma_{\rm L}t_{\rm a}+\gamma_{\rm S}t_{\rm b})} + {\rm e}^{-(\gamma_{\rm S}t_{\rm a}+\gamma_{\rm L}t_{\rm b})}}. \quad (5)$$

The aim of the present experiment is to measure this asymmetry in order to prove the existence of the interference and, therefore, that the two particles remain correlated despite their distance. The intensities of Eqs. (3) and (4) can be expressed as

$$I_{\rm like}(t_{\rm a},t_{\rm b}) = \frac{{\rm e}^{-2\gamma t}}{8}\{{\rm e}^{-\gamma_{\rm S}|t_{\rm a}-t_{\rm b}|} + {\rm e}^{-\gamma_{\rm L}|t_{\rm a}-t_{\rm b}|} - 2{\rm e}^{-\gamma|t_{\rm a}-t_{\rm b}|}\cos[\Delta m(t_{\rm a}-t_{\rm b})]\}, \quad (6)$$

$$I_{\rm unlike}(t_{\rm a},t_{\rm b}) = \frac{{\rm e}^{-2\gamma t}}{8}\{{\rm e}^{-\gamma_{\rm S}|t_{\rm a}-t_{\rm b}|} + {\rm e}^{-\gamma_{\rm L}|t_{\rm a}-t_{\rm b}|} + 2{\rm e}^{-\gamma|t_{\rm a}-t_{\rm b}|}\cos[\Delta m(t_{\rm a}-t_{\rm b})]\}, \quad (7)$$

with $t = t_{\rm a}$ (for $t_{\rm a} < t_{\rm b}$) or $t = t_{\rm b}$ (for $t_{\rm a} > t_{\rm b}$); their dependence on ($t_{\rm a}$- $t_{\rm b}$) is shown in Fig. 1.

Similarly, for a $J^{PC} = 0^{++}$ or 2^{++} symmetric state, one writes:

$$|\Psi(0,0)\rangle = \frac{1}{\sqrt{2}}[|\mathrm{K^0}(0)\rangle_{\rm a}|\overline{\mathrm{K}}^0(0)\rangle_{\rm b} + |\overline{\mathrm{K}}^0(0)\rangle_{\rm a}|\mathrm{K^0}(0)\rangle_{\rm b}], \text{ or}$$

$$|\Psi(0,0)\rangle = \frac{1}{\sqrt{2}}[|\mathrm{K_S}(0)\rangle_\mathrm{a}|\mathrm{K_S}(0)\rangle_\mathrm{b} - |\mathrm{K_L}(0)\rangle_\mathrm{a}|\mathrm{K_L}(0)\rangle_\mathrm{b}]. \quad (8)$$

The intensities become:

– $J^{PC} = 0^{++}$ or 2^{++}, like-strangeness events ($\mathrm{K^0K^0}$ or $\overline{\mathrm{K}}^0\overline{\mathrm{K}}^0$),

$$I_\mathrm{like}(t_\mathrm{a}, t_\mathrm{b}) = \frac{1}{8}\{\mathrm{e}^{-\gamma_\mathrm{S}(t_\mathrm{a}+t_\mathrm{b})} + \mathrm{e}^{-\gamma_\mathrm{L}(t_\mathrm{a}+t_\mathrm{b})} - 2\mathrm{e}^{-\gamma(t_\mathrm{a}+t_\mathrm{b})}\cos[\Delta m(t_\mathrm{a}+t_\mathrm{b})]\}; \quad (9)$$

– $J^{PC} = 0^{++}$ or 2^{++}, unlike-strangeness events ($\mathrm{K^0}\overline{\mathrm{K}}^0$ or $\overline{\mathrm{K}}^0\mathrm{K^0}$),

$$I_\mathrm{unlike}(t_\mathrm{a}, t_\mathrm{b}) = \frac{1}{8}\{\mathrm{e}^{-\gamma_\mathrm{S}(t_\mathrm{a}+t_\mathrm{b})} + \mathrm{e}^{-\gamma_\mathrm{L}(t_\mathrm{a}+t_\mathrm{b})} + 2\mathrm{e}^{-\gamma(t_\mathrm{a}+t_\mathrm{b})}\cos[\Delta m(t_\mathrm{a}+t_\mathrm{b})]\}. \quad (10)$$

Equations (9) and (10) can be compared with Eqs. (3) and (4). Again, there is an interference term with opposite sign for the two cases (unlike and like), but it oscillates with $(t_\mathrm{a} + t_\mathrm{b})$ instead of $(t_\mathrm{a} - t_\mathrm{b})$ and rapidly becomes negligible. These intensities never vanish after the $\mathrm{K^0}\overline{\mathrm{K}}^0$ creation.

3 Experimental method

3.1 Apparatus

The measurement was performed at the Low-Energy Antiproton Ring (LEAR) at CERN with the CPLEAR detector [17], shown in Figs. 2a – 2d. The 200 MeV/c antiprotons were extracted from LEAR with an intensity of 10^6 particles per second and stopped inside a 27-bar hydrogen gas target. A cylindrical tracking detector was located inside a solenoid (1 m radius, 3.6 m long) providing a 0.44 T magnetic field parallel to the beam. It consisted of two layers of MWPCs (PC1, PC2), six layers of drift chambers and two layers of streamer tubes. A hodoscope of 32 threshold Cherenkov counters sandwiched between two scintillator hodoscopes (S1, S2) provided charged-particle identification (Cherenkov light, time of flight and energy loss). The cylindrical target (11 mm radius) was surrounded by a small cylindrical proportional chamber PC0 (15 mm radius, 1 mm pitch, $> 99.5\%$ efficiency), see Fig. 2c. A thin silicon detector in front of the target entrance window (Fig. 2d) ensured the presence of an incoming antiproton, thus rejecting background events resulting from interactions in the target support structure.

The $\mathrm{K^0}\overline{\mathrm{K}}^0$ pairs are produced by $\overline{\mathrm{p}}\mathrm{p}$ annihilation at rest with a branching fraction of 0.7% [18] and evolve in vacuum either as $\mathrm{K_S K_S}$ or $\mathrm{K_L K_L}$ or $\mathrm{K_S K_L}$ (Section 2). The kaons have a momentum of 800 MeV/c, corresponding to a $\mathrm{K_S}$ mean decay length of 4 cm.

$\mathrm{K_S K_S}$ and $\mathrm{K_L K_L}$ occur mainly from the $\overline{\mathrm{p}}\mathrm{p}$ state $^3\mathrm{P}_0$ or $^3\mathrm{P}_2$ ($J^{PC} = 0^{++}$ or 2^{++}) while $\mathrm{K_S K_L}$ occurs from the state $^3\mathrm{S}_1$ ($J^{PC} = 1^{--}$). The branching fractions for these channels depend on the hydrogen density. At 27 bar, the ratio

$$\frac{\mathrm{BR(K_S K_S)}}{\mathrm{BR(K_S K_L)}} = 0.037 \pm 0.002$$

was measured with the CPLEAR detector [19]. From that result, a branching fraction of 7.4% is deduced for the symmetric states $J^{PC} = 0^{++}$ or 2^{++}. Therefore the $\mathrm{K^0}\overline{\mathrm{K}}^0$ system is considered to be an antisymmetric $J^{PC} = 1^{--}$ state and a correction is applied to the final result accounting for the 7.4% contamination.

The experiment tests the correlations of Eqs. (6) and (7). In order to determine the strangeness content of the neutral kaons at a given proper time, two cylindrical absorbers were placed around the target behind PC0 (Fig. 2c), each one $\approx 5\%$ of an interaction length. The first was made of carbon, 2.5 cm thick and 25 cm long at a radius of 7 cm, covering an azimuthal

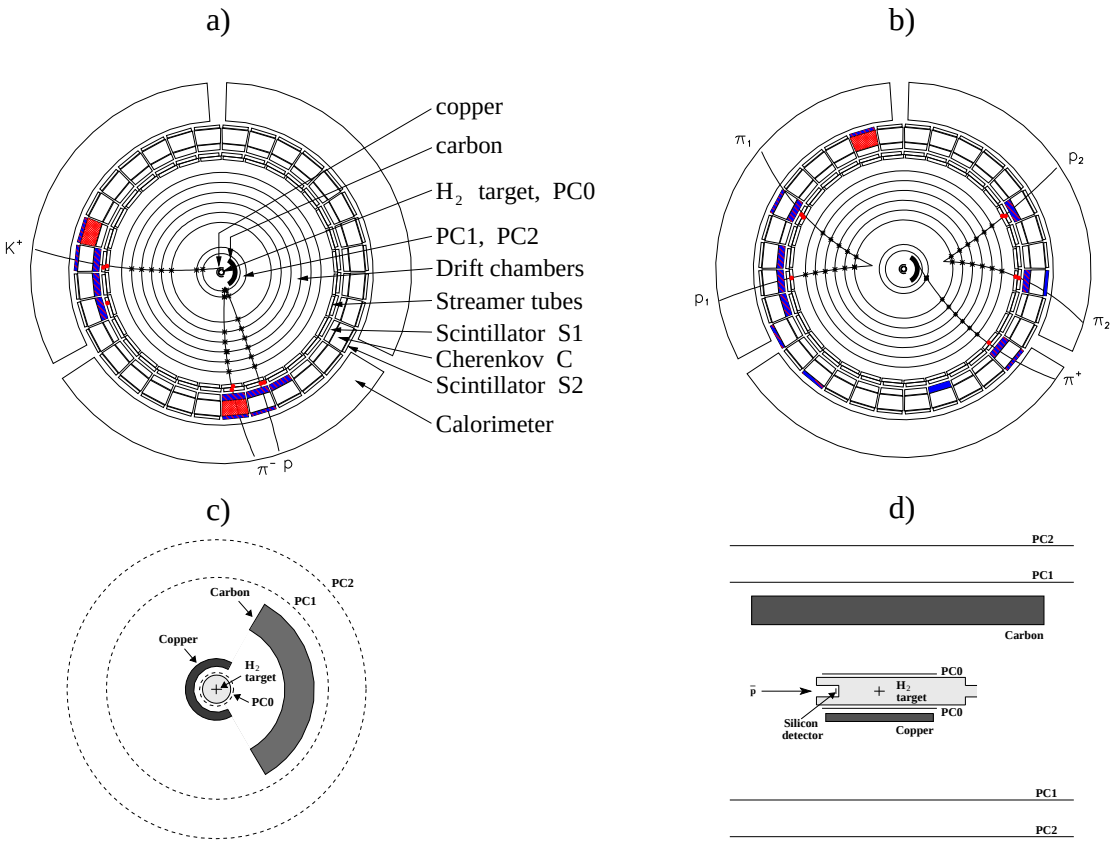

Figure 2: The CPLEAR detector (the magnet is not shown): full transverse view displaying a) a ΛK^+ event, b) a $\Lambda\Lambda$ event where one Λ extrapolates back to carbon and the other to copper (the extra π^+ is produced together with the Λ in carbon), and expanded c) transverse and d) side view of the central region showing the geometry of the absorbers.

angle of 115° in the transverse plane; it had been installed previously for measuring kaon regeneration in carbon [20]. The second absorber, made of copper, 0.7 cm thick and 10 cm long at a radius of 2 cm, covered most of the remaining angle (240°). The trigger required that no charged particles emerged out of the target (PC0 in veto) and that at least two charged tracks were detected by the tracking device.

The strangeness of the neutral kaons at the absorber position is determined by the strangeness of the state produced via strong interactions of either neutral kaons with the bound nucleons of the absorbers:

$$\mathrm{K}^0 + \text{nucleus} \rightarrow \mathrm{K}^+ + \mathrm{X}\ , \tag{11}$$

$$\overline{\mathrm{K}}^0 + \text{nucleus} \rightarrow \mathrm{K}^- + \mathrm{X}\ , \tag{12}$$

$$\overline{\mathrm{K}}^0 + \text{nucleus} \rightarrow \Lambda(\rightarrow \mathrm{p} + \pi^-) + \mathrm{X}\ , \tag{13}$$

thus the two neutral kaon final states considered are either $\mathrm{K}^+\Lambda$ unlike-strangeness events or $\mathrm{K}^-\Lambda$ and $\Lambda\Lambda$ like-strangeness events. Figure 3a shows the two possible experimental configurations. If the two back-to-back neutral kaons are produced within 30° of the vertical, both flight-paths cross the copper absorber. If they are produced within 60° of the horizontal, then one kaon crosses the copper and the other the carbon absorber. The first configuration is called C(0): both kaons have nearly equal proper times ($t_\mathrm{a} \approx t_\mathrm{b}$) when they interact in the absorber. The second configuration is called C(5): the flight-path difference is 5 cm on average, corresponding to a proper time difference $|t_\mathrm{a} - t_\mathrm{b}| \approx 1.2\ \tau_\mathrm{S}$. The intensity asymmetry is measured

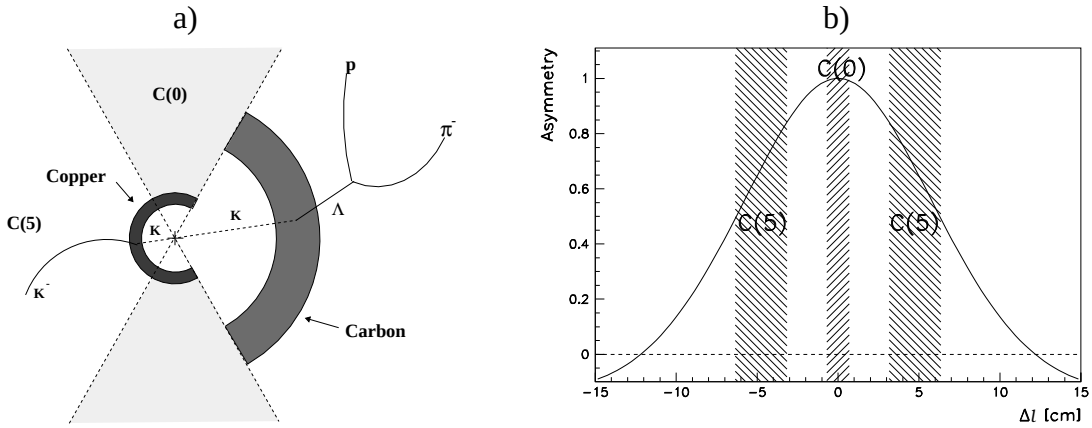

Figure 3: Conceptual sketch a) of the experiment with a $\Lambda\mathrm{K}^-$ event, and QM-predicted asymmetry b) $(I_{\mathrm{unlike}} - I_{\mathrm{like}})/(I_{\mathrm{unlike}} + I_{\mathrm{like}})$ as a function of the flight-path difference Δl. In b) the shaded areas are the regions of configurations C(0) and C(5). The horizontal dashed line is the prediction in the case of separability of the wave function (Furry).

for these two configurations. Figure 3b shows the corresponding QM predictions, Eq. (5), together with the flight-path intervals covered by the measurements. The C(0) configuration fulfils the conditions for an EPR-type experiment.

3.2 Strange-particle identification

The two-track events recorded are searched for a 1-V topology, i.e. at least one pair of opposite-charge tracks from a common vertex outside the PC0. The converted photons are rejected by a cut on the opening angle. In addition, the direction of the V momentum must cross one of the absorbers. The events, which contain at least either a $\mathrm{K_S} \to \pi^+ + \pi^-$ or a $\Lambda \to \mathrm{p} + \pi^-$ candidate, are further searched for additional Λ and $\mathrm{K}^\pm$ production.

– Λ *Selection.* The Λ selection requires that the positive track of the V has an S1-counter hit, that it gives no signal in the corresponding Cherenkov counter and that the $\mathrm{d}E/\mathrm{d}x$ in the S1 counter is compatible with the particle being a proton. The $\mathrm{K_S} \to \pi\pi$ contamination is eliminated by an invariant-mass cut based on the $\pi\pi$ hypothesis. Figure 4 shows the $\mathrm{p}\pi^-$ invariant-mass distribution. Events with masses between 1105 and 1125 MeV/c^2 are retained as Λs, with only a few per cent background.

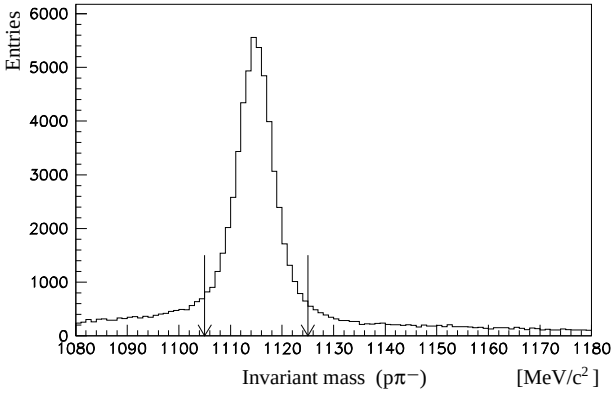

Figure 4: $\mathrm{p}\pi^-$ invariant-mass distribution. The arrows indicate the cut to select Λ.

– $\mathrm{K}^{\pm}$ *Selection.* A charged track, in order to be identified as $\mathrm{K}^{\pm}$, has to give an S1·S2 coincidence with no signal in the corresponding Cherenkov and has to cross one of the absorbers, see Fig. 2a. A lower momentum cut of 350 MeV/c ensures that a charged particle with a mass lower than a kaon has a velocity well above the Cherenkov threshold. Moreover this cut helps to reject charged kaons produced by low-momentum K^0 (non back-to-back) and also single pions from unreconstructed $\mathrm{K_S}$ decays.

4 Data analysis and results

A total of 8×10^7 events was recorded and analysed.

4.1 $\Lambda\mathrm{K}^+, \Lambda\mathrm{K}^-$ final states

In order to obtain the $\Lambda\mathrm{K}^+$ and $\Lambda\mathrm{K}^-$ final states, Eqs. (11–13), the Λ and $\mathrm{K}^{\pm}$ selection mentioned in Section 3.2 is applied. The intersections of the Λ and $\mathrm{K}^{\pm}$ trajectories with the absorber median planes determine the two corresponding interaction points, thus the directions of the two neutral kaons. A cut on the opening angle of the two reconstructed directions in the transverse plane selects the back-to-back kaon pairs. From the event distribution outside the cut, the contamination of non back-to-back events is evaluated to be ≈15%.

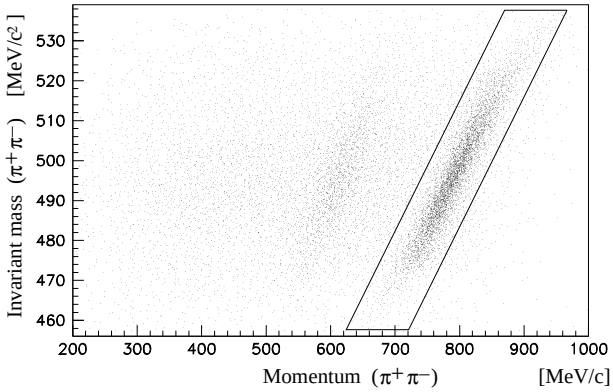

Figure 5: $\pi^+\pi^-$ invariant mass vs. momentum. The solid lines show the cuts to select 800 MeV/c $\mathrm{K_S}$.

When comparing the yield of $\Lambda\mathrm{K}^+$ and $\Lambda\mathrm{K}^-$ events, it is necessary to know the efficiency ratio $\eta = (\sigma_{\mathrm{K}^+} \times \varepsilon_{\mathrm{K}^+})/(\sigma_{\mathrm{K}^-} \times \varepsilon_{\mathrm{K}^-})$ where σ_{K^+} and σ_{K^-} are the cross-sections for reactions (11) and (12), and $\varepsilon_{\mathrm{K}^+}$ and $\varepsilon_{\mathrm{K}^-}$ the corresponding detection efficiencies. To measure η, a calibration data sample was used, consisting of $\overline{\mathrm{p}}\mathrm{p} \to \mathrm{K}^0\overline{\mathrm{K}}^0$ events where one neutral kaon was an 800-MeV/c $\mathrm{K_S}$ $(\to \pi^+\pi^-)$ and the other kaon (always 50% K^0 and 50% $\overline{\mathrm{K}}^0$) produced a charged kaon in the absorber. In Fig. 5 the scatter plot of the $\pi\pi$ invariant mass versus the momentum shows an accumulation around the K^0 mass with a mean momentum of 800 MeV/c corresponding to the back-to-back two-kaon production. A strong mass–momentum correlation can be seen as a result of momentum resolution. Events within the enclosed area were retained as $\mathrm{K_S}$ from back-to-back $\mathrm{K}^0\overline{\mathrm{K}}^0$ events. For each absorber the ratio of the number of detected K^+ to K^- events associated with these $\mathrm{K_S}$ is a direct measurement of the efficiency ratio η.

The $\mathrm{K}^{\pm}$ mass squared M^2 is determined from the measured $\mathrm{d}E/\mathrm{d}x$ and momentum, and its distribution is shown in Fig. 6a for the calibration data sample. The few remaining pions are tracks which escaped the Cherenkov counter. The large (recoil) proton signal is related to neutral-kaon quasi-elastic scattering in the absorbers. By cutting on the time of flight, most of the protons and pions are rejected (Fig. 6b). Figure 6c shows the same distribution with a cut on the χ^2 of $\mathrm{d}E/\mathrm{d}x$. The ratio of the number of K^+ events to the number of K^- events, when all cuts are included, gives $\eta_{\mathrm{Cu}} = 1.64 \pm 0.06$ for copper and $\eta_{\mathrm{C}} = 1.60 \pm 0.08$ for carbon.

For the $\Lambda\mathrm{K}^{\pm}$ events the $\mathrm{K}^{\pm}$ mass-squared distributions are shown in Figs. 6d – 6f, and indicate that the $\Lambda\mathrm{K}^-$ like-strangeness events are largely suppressed. The $\mathrm{K}^{\pm}$ mass distributions with the final cuts are given in Fig. 7, separately for each configuration, C(0) and C(5). The measured numbers of $\Lambda\mathrm{K}^-$ and $\Lambda\mathrm{K}^+$ events, obtained from these plots,

$$N_{\Lambda\mathrm{K}^-} = 1,\ N_{\Lambda\mathrm{K}^+} = 16 \quad \text{for C(0)},$$

$$N_{\Lambda\mathrm{K}^-} = 12,\ N_{\Lambda\mathrm{K}^+} = 54 \quad \text{for C(5)},$$

and corrected with the measured efficiency ratios, lead to the intensity asymmetry values, Eq. (5),

$$A(0) = 0.81 \pm 0.17 \quad \text{for C(0)},$$

$$A(5) = 0.48 \pm 0.12 \quad \text{for C(5)}.$$

The QM prediction of the asymmetry, Eq. (5), was calculated taking account of the variation of the flight paths due to the absorber thickness and to the size of the annihilation region inside the target. The calculation was performed by simulating the stopped $\overline{\mathrm{p}}$ distribution in space, the isotropic $\mathrm{K}^0\overline{\mathrm{K}}^0$ production and the interaction points within the absorbers, and weighting the events according to Eqs. (3) and (4). The contribution of the 7.4% of $\mathrm{K}^0\overline{\mathrm{K}}^0$ pairs in a symmetric state was accounted according to Eqs. (9) and (10). The contribution of the estimated 15% of non back-to-back events was also included.

The calculation results, $A^{\mathrm{QM}}(0) = 0.93$ and $A^{\mathrm{QM}}(5) = 0.56$, are in agreement with the above measured values. If the wave function were separable as suggested by Furry [2], then the asymmetry A would be equal to 0 for both configurations, regardless of the amount of background. This value is excluded with a CL $> 99.99\%$.

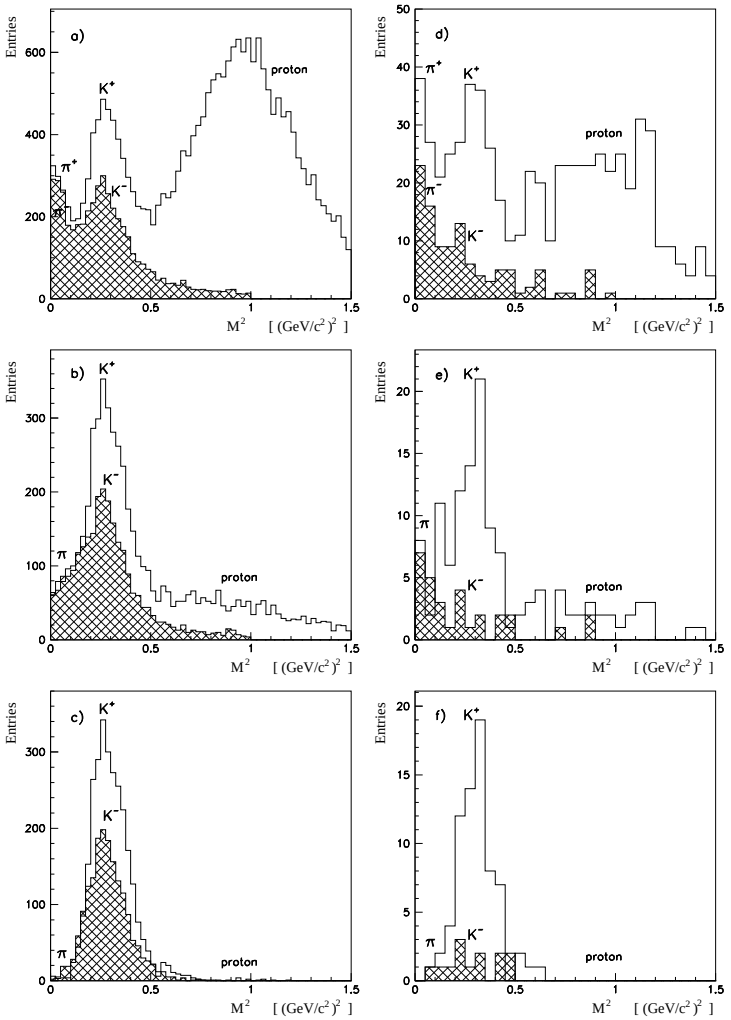

Figure 6: $\mathrm{K}^{\pm}$ mass-squared distributions for the $\mathrm{K_S K}^{\pm}$ calibration events: a) all candidates, b) time-of-flight cut, c) $\mathrm{d}E/\mathrm{d}x$-χ^2 cut. Also shown are the distributions for the $\Lambda\mathrm{K}^{\pm}$ events, with the same cuts: d) – f).

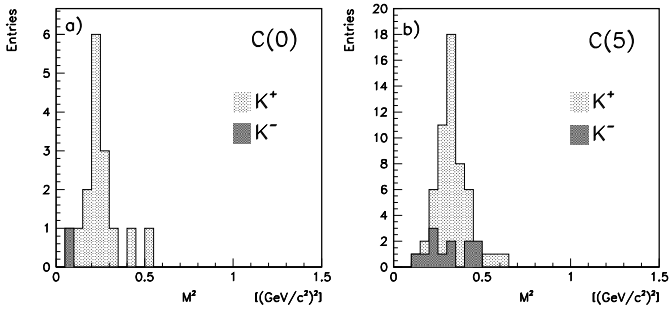

Figure 7: $\mathrm{K}^{\pm}$ mass-squared distribution of the $\Lambda\mathrm{K}^{\pm}$ final sample for a) C(0) and b) C(5) configurations.

4.2 $\Lambda\Lambda$ final states

Like-strangeness final states are also produced when both neutral kaons interact to produce Λ in the absorbers (Fig. 2b). Figure 8 shows the scatter plots of the two $\mathrm{p}\pi^-$ invariant masses for the C(0) and C(5) configurations. A significant signal is only seen for the C(5) configuration. Taking account of the background estimated from the events outside the selected Λ mass region, the values of the measured yield $N_{\Lambda\Lambda}$ are 1 ± 1 for C(0) and 5 ± 2 for C(5).

The expected number of $\Lambda\Lambda$ like-strangeness events was calculated from the measured number of single-Λ events for two different hypotheses: with interference, according to Eq. (3), and without interference. The probability for a $\overline{\mathrm{K}}^0$ to produce a detectable Λ was measured by comparing the production of Λs associated with a 800-MeV/c $\mathrm{K_S}$ to single-$\mathrm{K_S}$ production, and the corrections due to the topological differences were evaluated. The calculation included the estimated number of single Λ produced by non back-to-back $\mathrm{K}^0\overline{\mathrm{K}}^0$ pairs (an equal amount of symmetric and antisymmetric states was assumed).

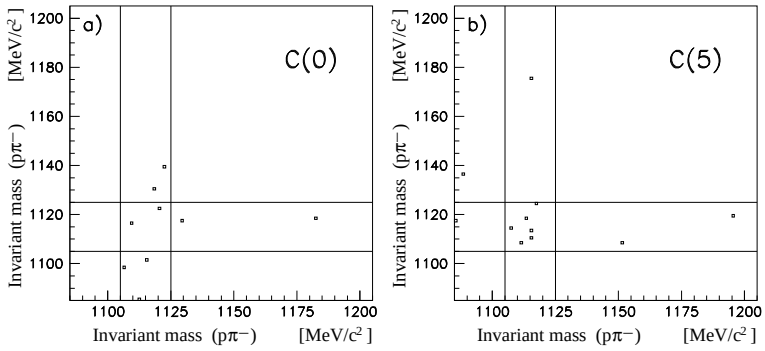

Figure 8: Invariant-mass scatter plot of one of the $\mathrm{p}\pi^-$ pair vs. the other for a) C(0) and b) C(5) configurations. The lines at (1115 ± 10) MeV/c^2 correspond to the Λ mass cuts.

As a result, if the interference predicted by Eq. (3) is correct, the values of the expected yield $N_{\Lambda\Lambda}^{\mathrm{QM}}$ are 2.1 ± 0.4 for the C(0) configuration and 10.2 ± 1.5 for the C(5) configuration. In the case of no interference, these numbers become respectively 16.8 ± 3.1 and 16.0 ± 2.7, thus the values of $N_{\Lambda\Lambda}$ reported above strongly favour the QM-predicted strangeness correlation.

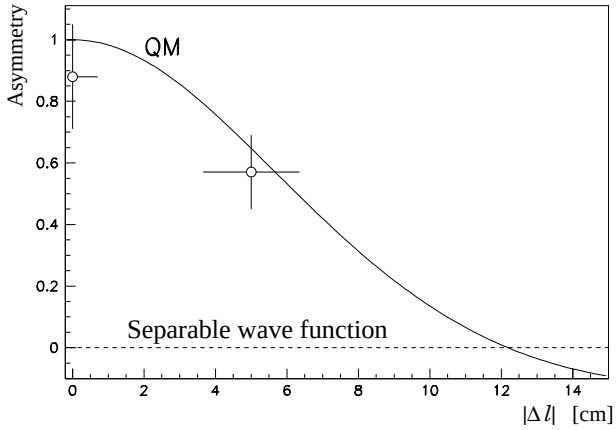

Figure 9: Asymmetry of the measured $\Lambda\mathrm{K}^{\pm}$ yields after background subtraction, for the two experimental configurations. The solid curve is the QM prediction. The dashed line is the prediction for a separable wave function.

5 Conclusion

Strangeness correlations of $\mathrm{K^0\overline{K}^0}$ were measured far away from the production point. The neutral kaons were produced in $\mathrm{p\overline{p}}$ annihilations at rest mainly in a $J^{PC} = 1^{--}$ state. Two experimental configurations were studied corresponding to 0 and $\approx 1.2\ \tau_{\mathrm{S}}$ proper time difference between the two strangeness measurements. The configuration with zero time difference fulfils the conditions of an EPR-type experiment. In both cases, the asymmetries of the yields for unlike- and like-strangeness events ($\Lambda\mathrm{K^+}$ and $\Lambda\mathrm{K^-}$, respectively) are consistent with the values predicted from QM and therefore with the non-separability hypothesis of the $\mathrm{K^0\overline{K}^0}$ wave function. These results are summarized in Fig. 9. The non-separability hypothesis is also strongly favoured by the yield of $\Lambda\Lambda$ events. The probability of satisfying the separability hypothesis of Furry is less than 10^{-4}.

Acknowledgements

We are grateful to Abner Shimony for his comments on this paper. We would like to thank the CERN LEAR staff for their support and co-operation, as well as the technical and engineering staff of our institutes. This work was supported by the following institutions: the French CNRS/Institut de Physique Nucléaire et de Physique des Particules, the French Commissariat à l'Energie Atomique, the Greek General Secretariat of Research and Technology, the Netherlands Foundation for Fundamental Research on Matter (FOM), the Portuguese JNICT, the Ministry of Science and Technology of the Republic of Slovenia, the Swedish Natural Science Research Council, the Swiss National Science Foundation, the UK Particle Physics and Astronomy Research Council (PPARC), and the US National Science Foundation.

References

[1] A. Einstein, B. Podolsky and N. Rosen, Phys. Rev. 47 (1935) 777.
[2] W.H. Furry, Phys. Rev. 49 (1936) 393.
[3] L. de Broglie, C.R. Acad. Sci. (France) 183 (1926) 447.
[4] D. Bohm, Phys. Rev. 85 (1952) 166, 180.
[5] J.S. Bell, Physics 1 (1964) 195.
[6] J.F. Clauser, M.A. Horne, A. Shimony and R.A. Holt, Phys. Rev. Lett. 23 (1969) 880.
[7] S.J. Freedman and J.F. Clauser, Phys. Rev. Lett. 28 (1972) 938.
[8] A. Aspect, P. Grangier, G. Roger, Phys. Rev. Lett. 47 (1981) 460; A. Aspect, P. Grangier, G. Roger, Phys. Rev. Lett. 49 (1982) 91; A. Aspect, J. Dalibard, G.Roger, Phys. Rev. Lett. 49 (1982) 1804.
[9] T.E. Kiess, Y.H. Shih, A.V. Segienko and C.O. Alley, Phys. Rev. Lett. 71 (1993) 3893 and references therein.
[10] W. Tittel et al., Phys. Rev. Lett., in print.
[11] G.C. Ghirardi, R. Grassi, R. Ragazzon, in DAΦNE Physics Handbook, eds. L. Maiani et al. (LNF, Frascati, 1992) p. 283.
[12] D.R. Inglis, Rev. Mod. Phys. 33 (1961) 1.
[13] H.J. Lipkin, Phys. Rev. 176 (1968) 1715.
[14] J. Six, Phys. Lett. B 114 (1982) 200; J.Six in Proc. of the Third LEAR Workshop (Tignes, 1985), eds. U. Gastaldi et al. (Editions Frontières, Gif-sur-Yvette, 1985) p. 511.
[15] F. Selleri, Lett. Nuovo Cim. 36 (1983) 521; F. Selleri, Phys. Rev. A 56 (1997) 3493.
[16] A. Muller, Quantum Mechanics and locality in the $\mathrm{K^0\overline{K}^0}$ system. Experimental verification possibilities, Saclay Int. Rep. DAPNIA/SPP (94–36), 1994.
[17] R. Adler et al., CPLEAR Collaboration, Nucl. Instrum. Methods A 379 (1996) 76.

[18] R. Armenteros and B. French, Antinucleon–Nucleon Interactions, in: High Energy Physics, vol. IV, ed. E.H.S. Burhop (Academic Press, New York, 1969) p. 311.
[19] R. Adler et al., CPLEAR Collaboration, Phys. Lett. B 403 (1997) 383.
[20] A. Angelopoulos et al., CPLEAR Collaboration, Phys. Lett. B 413 (1997) 422.